

Automated screening of congestive heart failure using variational mode decomposition and texture features extracted from ultrasound images

U. Raghavendra¹ · U. Rajendra Acharya^{2,3,4} · Anjan Gudigar¹ · Ranjan Shetty⁵ · N. Krishnananda⁶ · Umesh Pai⁶ · Jyothi Samanth⁶ · Chaithra Nayak⁶

Received: 2 November 2016 / Accepted: 5 January 2017
© The Natural Computing Applications Forum 2017

Abstract Heart is an important and hardest working muscular organ of the human body. Inability of the heart to restore normal perfusion to the entire body refers to cardiac failure, which then with symptoms results in manifestation of congestive heart failure (CHF). Impairment in systolic function associated with chronic dilation of left ventricle is referred as dilated cardiomyopathy (DCM). The clinical examination, surface electrocardiogram (ECG), chest X-ray, blood markers and echocardiography play major role in the diagnosis of CHF. Though the ECG manifests chamber enlargement changes, it does not possess sensitive marker for the diagnosis of DCM, whereas echocardiographic assessment can effectively reveal the presence of asymptomatic DCM. This work proposes an automated screening method for classifying normal and CHF echocardiographic images affected due to DCM using variational mode decomposition technique. The texture

features are extracted from variational mode decomposed image. These features are selected using particle swarm optimization and classified using support vector machine classifier with different kernel functions. We have validated our experiment using 300 four-chamber echocardiography images (150: normal, 150: CHF) obtained from 50 normal and 50 CHF patients. Our proposed approach yielded maximum average accuracy, sensitivity and specificity of 99.33%, 98.66% and 100%, respectively, using ten features. Thus, the developed diagnosis system can effectively detect CHF in its early stage using ultrasound images and aid the clinicians in their diagnosis.

Keywords Congestive heart failure · Dilated cardiomyopathy · Machine learning · Texture features · VMD

✉ U. Raghavendra
raghavendra.u@manipal.edu

¹ Department of Instrumentation and Control Engineering, Manipal Institute of Technology, Manipal University, Manipal 576104, India

² Department of Electronics and Computer Engineering, Ngee Ann Polytechnic, Singapore 599489, Singapore

³ Department of Biomedical Engineering, School of Science and Technology, SIM University, Singapore 599491, Singapore

⁴ Department of Biomedical Engineering, Faculty of Engineering, University of Malaya, Kuala Lumpur, Malaysia

⁵ Department of Cardiology, Kasturba Medical College and Hospital, Manipal University, Manipal 576104, India

⁶ Department of Cardiovascular Technology, School of Allied Health Sciences, Manipal University, Manipal 576104, India

1 Introduction

Heart is one of the vital organs which pumps blood to the whole body tissue in order to provide oxygen. Adequate pumping of heart is necessary for healthy living. According to European Heart Network and European Society of Cardiology, nearly 4 million people die due to cardiovascular diseases in Europe and 1.9 million in European Union (EU) [1]. Cardiovascular disease widely ranges from genetic disorder to acquired heart diseases [2]. Heart failure is the most common syndrome that results in death if left untreated. Etiologic basis for congestive cardiac failure possesses trends of multiple components with respect to structural heart disease, ischemic heart disease, congenital heart disease, myocardial disease, valvular heart disease, systemic diseases, etc. that manifest clinical symptoms of failure. Dilated

cardiomyopathy (DCM) is one of the myocardial diseases that can precipitate into congestive heart failure (CHF) as it progresses. In DCM, dysfunctional myocardium undergoes chronic dilatation as the result of remodeling [3]. This enhances required stroke volume ejection by the left ventricle; however, the ejection fraction declines as the disease progresses. At this stage, patient may possess exertional symptoms of breathlessness and may limit the routine activity [3]. Patient develops the CHF once the latent myocardial damage reaches decompensated stage which is manifested clinically by the presence of symptoms at rest. CHF results in deterioration of subject's vital hemodynamics and precipitates into extreme breathlessness in supine position, sweating, hemoptysis, chest pain and signs of pulmonary edema [3]. Complete physical examination, electrocardiogram (ECG) and chest X-ray play major role in assessing the patient's condition and hemodynamics preferably in symptomatic subjects. ECG is a noninvasive method which shows irregularities in the heart beat and adds certain diagnostic features in assessing the function and disorders of cardiovascular system [4]. In addition, lack of physicians and advanced methodologies, automated detection and diagnosis using ECG samples have attracted research community to develop computer-aided diagnosis (CAD) tools to assist the clinicians to validate their decisions.

ECG-based CAD system uses samples collected from the ECG for the analysis, and it has become a gold standard in developing the CAD tools for CHF [4]. Many of these techniques use machine learning algorithms with feature extraction to differentiate the ECG signals. Also, feature selection scheme is used to enhance the classifier performance. Asyali [5] has used Bayesian classifier with linear discriminant analysis and achieved a performance of 93.24%. The k-nearest neighbor classifier along with genetic algorithms used by Isler and Kuntalp [6] achieved an accuracy of 96.39%. In [7], wavelet decomposition and soft decision technique did not achieve remarkable success (accuracy is 88.6%). In [8], combination of short-term heart rate variability (HRV) and regression tree resulted 89.7% sensitivity and 100% specificity. Yu and Lee [9] showed reasonable success (accuracy) of 97.59% by using support vector machine (SVM) and conditional mutual information feature selector (CMIFS). Masetic and Subasi [10] have used autoregressive Burg method and achieved 100% classification success. Recently, Acharya et al. [11] have used empirical mode decomposition for the characterization of congestive heart failure based on heart rate signals. They have achieved a maximum accuracy of 97.64%.

Though several CAD tools are presented in the literature using ECG signals, subjects with non-ischemic dilated cardiomyopathy may or may not indicate the

symptoms of CHF in ECG. But the diagnosis can be done accurately by echocardiography examination and it can also diagnose the DCM in asymptomatic subjects [2]. The echocardiography-based diagnostic tool for the identification of non-ischemic DCM includes dilated left ventricle, globally reduced ventricular wall contraction, reduced ventricular ejection fraction and right heart failure in the end stage. In addition to diagnosing DCM, echocardiography can reveal the structural heart disease that would precipitate into ventricular dysfunction [12]. Hence, the newer guideline recommends echocardiographic examination in subjects who are at risk [2]. Echocardiography helps in the identification of DCM in its early asymptomatic stage which needs immediate medical attention for the therapy [13]. Echocardiography is a diagnostic procedure where the subject's heart is assessed with respect to its structure and function. The test yields the high diagnostic accuracy in assessing the patients with CHF. ECG can still be beneficial in therapeutic decision and prognostication, whereas this does not convey any specific diagnostic criteria for DCM [14–16]. Thus, echocardiography plays a major role in assessing patients with CHF with respect to defining its etiology. DCM can switch from asymptomatic to symptomatic CHF stage which may be assessed by echocardiography. The ability to detect DCM in its asymptomatic stage holds the best indication for echocardiographic test. Applying this information will direct the subjects for medical attention for therapy and follow-up. Echocardiography can also provide information on ventricular function, associated lesions and structural heart disease that cannot be explored by just 12-lead ECG [17]. By observing the above limitations of ECG, this work proposes an efficient methodology for the analysis of CHF caused due to DCM using echocardiography images. To the best of our knowledge, this is the first attempt in developing CAD system for the analysis of CHF using echocardiography images.

The proposed method involves four stages, namely data preprocessing, image decomposition, feature extraction, feature optimization and classification. Initially, the original images are subjected to variational mode decomposition (VMD). VMD decomposes an original image into its principal components, which can efficiently represents unique patterns of CHF which are very close in their original representation over normal subjects. Also, it has an ability to separate subjects which has moved from asymptomatic to symptomatic CHF stage. Then, texture features are extracted from the VMD images. Further, particle swarm optimization (PSO) and support vector machine (SVM) classification model are combined to obtain the optimized features. The graphical representation of the proposed scheme is shown in Fig. 1.

2 Materials and methods

2.1 Data acquisition

Echocardiography images from 100 subjects (50 normal and 50 CHF) were obtained based on signs and symptoms of CHF and assessment of left ventricular ejection fraction (LVEF) from an experienced cardiophysician. Ejection fraction is a measure of left ventricular systolic function denoted by ratio of the stroke volume ejected each beat to end diastolic volume. $LVEF < 45\%$ carries considerable adverse outcome among patients with CHF [18]. Hence, present study included patients with CHF having $LVEF < 45\%$ and age-matched healthy volunteered controls. Ethical clearance has taken from the institute ethical committee, and the control subjects were the normal individuals who appeared for routine health checkup. Echocardiography examination was performed using VIVID E7 dimension GE healthcare system. Complete echocardiography examination was performed, and left ventricle DICOM image of four-chamber view was stored. These normal and CHF DICOM sequences were converted to JPEG image format with a resolution of 600×800 . Three image samples were selected from every subjects (one from the center, one from 20 images before and after the center image) for this study. The details of age, sex and number of subjects in each class are given in Table 1. Figure 2 shows the typical normal and CHF ultrasound images used in this study.

2.2 Data preprocessing

Preprocessing is very important step to get an accurate result in the classification problem. Initially, all the images are subjected to adaptive histogram equalization in order to enhance the contrast [19] and morphological operators with disk = 5 [25], to remove the aforementioned information. Further, connected component analysis is performed to generate the bounding box around the four-chamber heart.

2.3 Variational mode decomposition (VMD)

The four-chamber echocardiography images taken from normal and CHF subjects are visually non-separable. The conventional bidirectional decomposition methods such as wavelet, Gabor, shearlet, curvelet are may not be suitable as they are not adaptive corresponding to the signal [21]. Also, they represent various image components by the same frequency spectrum. Hence, this paper uses two-dimensional (2D) VMD which adaptively decomposes an input image into k discrete number of spectral bands. 2D VMD is similar to 1D VMD and minimizes the bandwidth of the sub-signals or modes while retaining data fidelity. In frequency domain, 2D analytic signal can be expressed as [21],

$$\hat{\mu}_{AS,k}(\omega) = (1 + \text{sgn}(\omega, \omega_k)) \hat{\mu}_k(\omega) \quad (1)$$

Then, the functional to be minimized to find the optimal μ_k in the Fourier domain is given by,

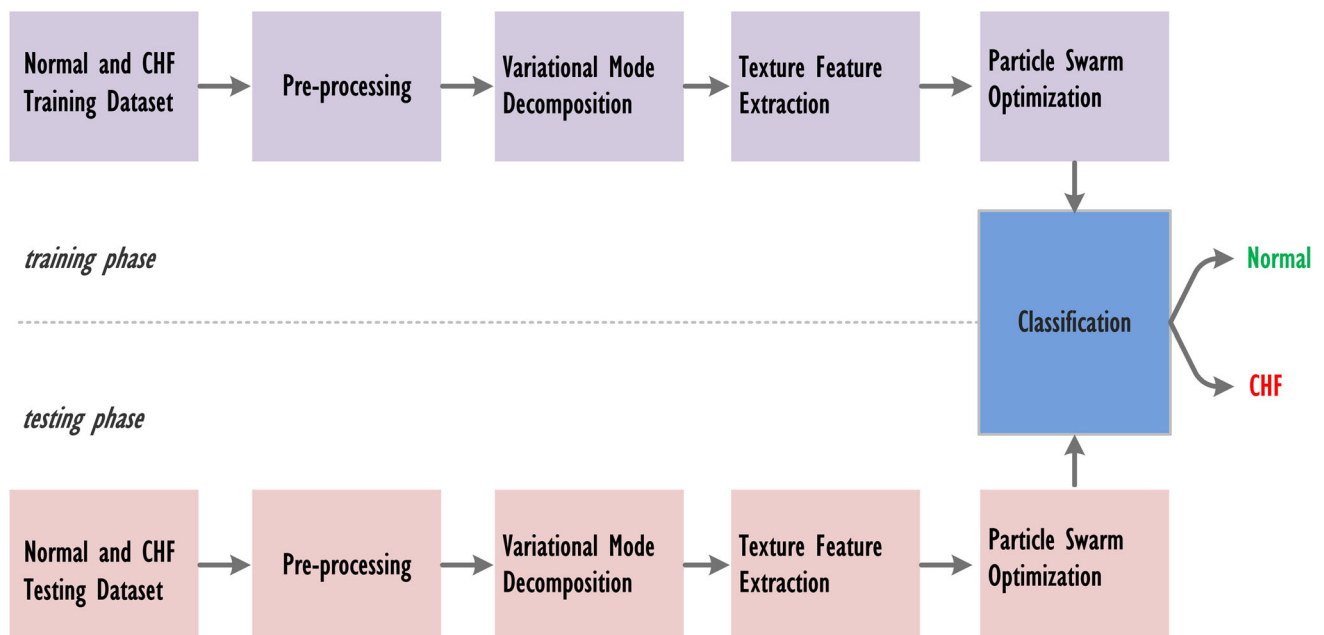
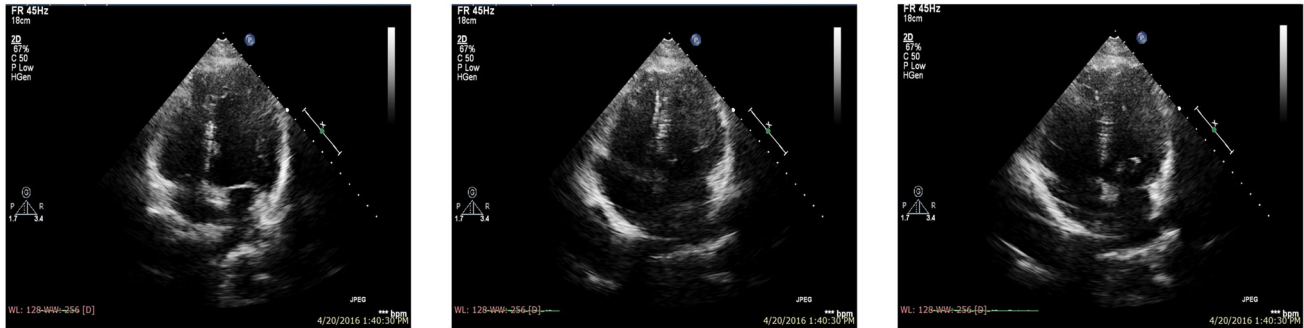


Fig. 1 Graphical representation of the proposed algorithm

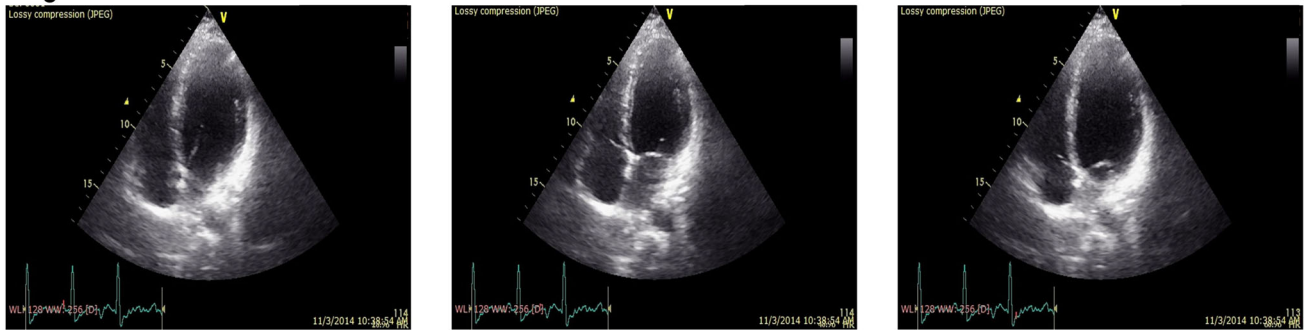
Table 1 Details of data used in this study

Categories	No. of samples	No. of male patients	No. of female patients	Age range (years)
Normal	150	35	15	28–79
CHF	150	32	18	08–79

Normal



Congestive Heart Failure

**Fig. 2** Typical ultrasound images of normal and CHF classes

$$\min_{\mu_k, \omega_k} \left\{ \sum_k \alpha_k \left\| \nabla \left[\mu_{AS,k}(x) e^{-j(\omega_k x)} \right] \right\|_2^2 \right\} \quad (2)$$

$$\text{s.t. } \forall x : \sum_k \mu_k(x) = f(x)$$

where f is a signal, μ is its mode, ω is the frequency, $k = 1, \dots, K$ is number of modes, and α is bandwidth constraint. Further, the optimization is done using alternate direction method of multipliers (ADMM) [22–24]. Thus, using Lagrangian multiplier (λ) into the quadratic penalty term, Eq. (2) can be simplified as,

$$\sum_k \alpha_k \left\| \nabla \left[\mu_{AS,k}(x) e^{-j(\omega_k x)} \right] \right\|_2^2 + \left\| f(x) - \sum_k \mu_k(x) + \frac{\lambda(x)}{2} \right\|_2^2 - \left\| \frac{\lambda(x)}{4} \right\|_2^2 \quad (3)$$

Further, the modes are updated by simple Wiener filtering, directly in Fourier domain with a filter tuned to the current

center frequency. Then, the center frequencies and the modes are updated. In this work, preprocessed images are resized to 64×64 using bicubic interpolation [20] and the 2D VMD is executed for the parameters $K = 5$ and $\alpha = 5000$ as shown in Fig. 3. 2D VMD is a fully adaptive non-recursive method which uses minimal parameters for decomposition. These adaptive decomposition results in different texture patterns for normal and CHF subjects as they depicts structural variation among them. These different patterns are shown in Fig. 3.

2.4 Texture feature extraction

Texture features describe various image properties such as regularity, coarseness and smoothness which basically represent mutual relationship among neighboring pixel intensities that are repeated over an area larger than the size of the relationship [26]. These properties play a vital role in pattern recognition and classification.

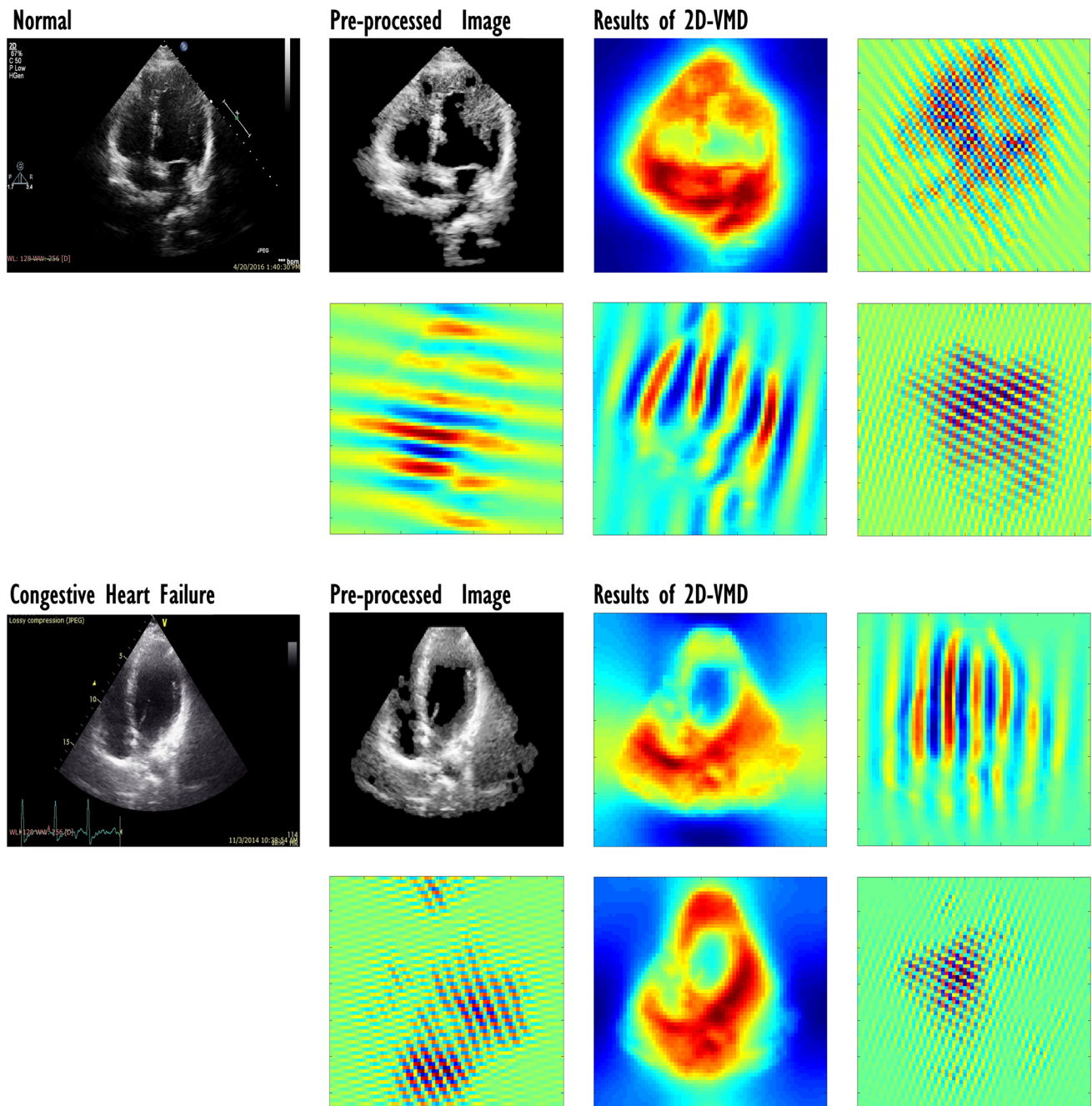


Fig. 3 Results of 2D VMD of normal and CHF images for five modes

2.4.1 Co-occurrence matrix

Gray-level co-occurrence matrix (GLCM) describes the possible combination of gray levels which often occur in a particular image. It also depicts the interrelation among neighboring pixels [26–29]. It computes various second-order statistical measures such as homogeneity ($f1$), contrast ($f2$), correlation ($f3$) and entropy ($f4$) [29, 30]. In addition, gray-level difference statistical measures can also be computed using difference vector. The obtained

difference vector can generate mean ($f5$), contrast ($f6$), entropy ($f7$) and angular second-order moments ($f8$) and their different variants [31].

2.4.2 Run length matrix

Run length matrix $P_{\theta}(i, j)$ depicts the successive appearance of i th gray level for j times with different orientation θ , where j is known as run length. Generally, the run length matrix will be computed for $\theta = 0^{\circ}, 45^{\circ}, 90^{\circ}$ and 135° in

order to determine following features [32]: long-run emphasis (f_9), short-run emphasis (f_{10}), gray-level non-uniformity (f_{11}), run percentage (f_{12}), run length non-uniformity (f_{13}) and their different variants.

2.5 Feature optimization and selection

2.5.1 Particle swarm optimization (PSO)

Particle swarm optimization (PSO) is an evolutionary computation method inspired by swarm intelligence [33, 34]. Generally PSO achieves objectives in a search space using personal as well as social behavior of the populations (swarms). The optimal solution is computed based on iteration using personal best position obtained in the previous iteration (p_{best}) and population best position (g_{best}) [33]. Consider particles $z_i = (z_{i1}, z_{i2}, \dots, z_{id})$, in a search space with dimension d . Each particle in the search space has the velocities $v_i = (v_{i1}, v_{i2}, \dots, v_{id})$. The PSO examines optimal solution by updating the position of the particles and its velocity using following equations

$$z_{id}^{t+1} = z_{id}^t + v_{id}^{t+1} \quad (4)$$

$$v_{id}^{t+1} = w * v_{id}^t + a_1 * r_1 * (p_{id} - z_{id}^t) + a_2 * r_2 * (p_{gd} - z_{id}^t) \quad (5)$$

where w is the inertia weight, a_1 and a_2 are acceleration constants, r_1 and r_2 are the uniformly distributed $U[0, 1]$ random values, and p_{id} and p_{gd} represent the p_{best} and g_{best} in dimension d . Moreover, PSO is terminated for the pre-defined maximum iterations or better fitness value.

2.5.2 Support vector machine (SVM)

SVM separates the class members by generating hyperplanes which are parallel to optimal hyperplanes [35]. Generally, SVM classifier is designed for two-class classification problem and it is less vulnerable to over fit. In case the features cannot be separated by a linear function, it will be mapped to the high-dimensional feature space using nonlinear kernel functions. In our study, we have used different kernel functions for the analysis.

Polynomial function of degree d is given by

$$K(x_i, x_j) = (1 + x_i' x_j)^d \quad (6)$$

where d is different polynomials [35].

RBF with variance σ^2 is given by,

$$K(x_i, x_j) = e^{-\frac{\|x_i - x_j\|^2}{2\sigma^2}} \quad (7)$$

We have also used statistically efficient tenfold cross-validation technique to build this classification model [36]. In this, complete dataset is roughly divided into ten partitions

(folds). Each time, one portion is used for testing and left over nine portions are used for training the model. The average of different statistical measures such as accuracy, sensitivity, specificity and positive predictive value (PPV) of all tenfold is computed to evaluate the performance of the system.

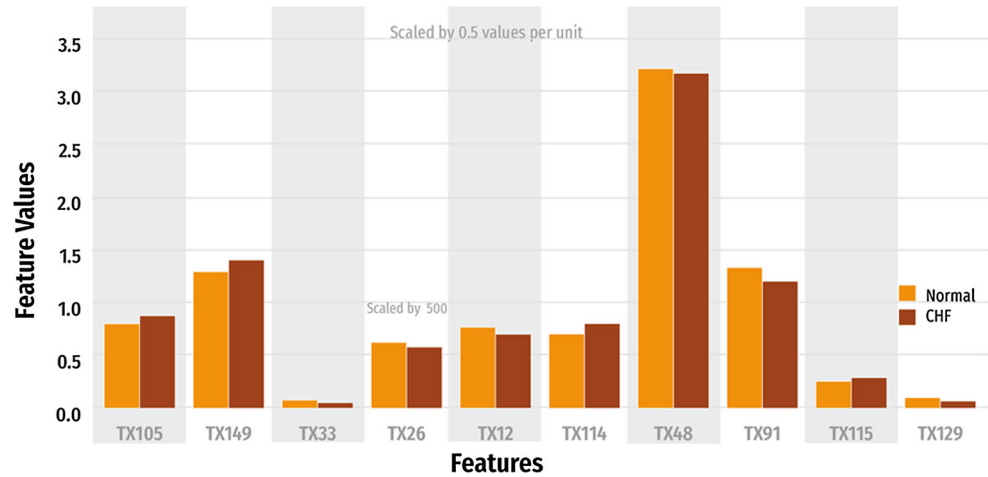
2.5.3 Combination of PSO and SVM

This section provides the details of the combination of PSO and SVM in order to select the best minimum features with maximum performance. Initially, every single particle is initialized in a defined dimensional space with random position. Next, the fitness of the particle is evaluated using SVM. In this study, we have used classification accuracy as a fitness measure. Further, the position vector of the best particle will be saved as a better fitness. Likewise, for the global best the position vector is saved, if particle's fitness is better than the global fitness. Finally, the position and velocity of the particle are updated iteratively until stopping condition is satisfied [37]. In this work, we have used tenfold cross-validation scheme to select the features. Thus, the ratio of testing samples to training sample was kept nearly 1:9. The program is executed 10 times to enable each part of the data can take part in both training and testing phases.

3 Experimental results

The input images are decomposed using VMD up to scale five. Various texture features such as mean, contrast, entropy, angular second-order moments, long-run emphasis, short-run emphasis, gray-level non-uniformity, run percentage and run length non-uniformity are extracted from the decomposed VMD coefficients yielding $30 \times 5 = 150$ texture features. These features are optimized using PSO to obtain maximum performance with minimum number of features. In this work, we have used a set of 5, 10, 15 and 20 features using PSO. In this experiment, SVM classifier with different kernels such as polynomial of order 1, 2, 3 and radial basis function (RBF) are used. The mean value of the best ten texture features (TX105, TX149, TX33, TX26, TX12, TX114, TX48, TX91, TX115 and TX129) which are selected using PSO and SVM is shown in Fig. 4. The performance for SVM classifier with different kernel functions and various number of features are presented in Tables 2, 3, 4 and 5. Proposed method achieved highest performance of 99.33% accuracy, 98.66% sensitivity, 100% specificity and 100% PPV for polynomial (order 1) kernel using ten features. Table 6 shows the mean and standard deviation of the used ten features. Few other kernel functions also give similar

Fig. 4 Mean value of used texture features (TX) for two classes



high performances but with more number of features. Figure 5 shows the performance of the method using different features. Figure 6 shows the consolidated performance of four group of features for different kernel functions. It can be observed that the polynomial of order 1 and 2 have maintained consistent performance among different groups as compared to other kernel functions. The complete system is developed and tested under MATLAB environment.

4 Discussion

This paper presents an automated system for the characterization of normal and CHF subjects using echocardiography images. The proposed method can predict CHF in its early stage using VMD at its different scales as shown in Fig. 3. It decomposes an image into collective band-limited intrinsic mode functions [21], whereas used texture features can derive efficient and quantitative descriptions of textures among normal and CHF subjects [38, 39]. The combination of VMD and various texture features confirms its suitability in distinguishing two subjects using Ultrasound (US) images. It is very effective for minute structural variation while shifting from asymptomatic to symptomatic CHF stage. Figure 4 and Table 6 show that the majority of VMD features show smaller mean values for CHF subjects as compared to normal subjects, which helps to discriminate normal and CHF classes. In addition, extracted texture features coupled with the combination of PSO and SVM classifier with polynomial kernel (order 1) have achieved a maximum accuracy of 99.33% (shown in Table 3). Method achieved a maximum sensitivity of 98.66% which is comparable to the performance of other kernels. It can also be observed that VMD gives linear separation [21], whereas texture signifies the spatial distribution of gray

levels [38, 39]. Hence, VMD with texture provides discrimination between two classes using movements of four chambers. Proposed method is the first attempt in classifying normal and CHF echocardiography images using combination of PSO and SVM scheme. The experiment is repeated for different set of features (5, 10, 15 and 20) with various kernels. It is observed that our method produced maximum accuracy for a set of ten best features, whereas the performance will decline for increased set of features as shown in Fig. 6. Another advantage of the proposed method is utilizing tenfold cross-validation strategy [36]. Our method is also tested for threefold, fivefold and sevenfold cross-validation [40] and obtained the same results. We have found that the proposed method achieved a specificity of 100%, which signifies that the all normal subjects are correctly classified as normal. Hence, it reduces the workload of clinicians by 50%. Thus, they need to focus their attention only on CHF patients.

The proposed method availed a computation time of 0.0125 s during training and 0.0008 s for testing 300 US images using a system configuration of Core i5 with 4 GB RAM.

The salient characteristics of this CAD system are as follows:

1. It achieves a classification accuracy of 99.33% in classifying normal and CHF subjects.
2. It requires only ten features to achieve the highest performance and hence can be used as a standalone system.
3. Segmentation techniques are not needed, as the entire image is subjected for the analysis.
4. Detection of CHF at an early stage can help the patients to take suitable medication and hence save life.
5. It assists the clinicians by reducing their workload. Hence, it can be used in their daily screening.

Table 2 Performance evaluation using SVM classifier with different kernels using five features (ten iterations)

Kernel	TP	TN	FP	FN	Acc. (%)	PPV (%)	Sen. (%)	Spe. (%)
Poly order 1	143	150	0	7	97.66	100	95.33	100
Poly order 2	148	149	1	2	99	99.33	98.66	99.33
Poly order 3	145	149	1	5	98	99.31	96.66	99.33
RBF	135	141	9	15	92	93.75	90	94

TP true positive, *TN* true negative, *FP* false positive, *FN* false negative, *Acc.* accuracy, *PPV* positive predicted value, *Sen.* sensitivity, *Spe.* specificity

Table 3 Performance evaluation using SVM classifier with different kernels using ten features (ten iterations)

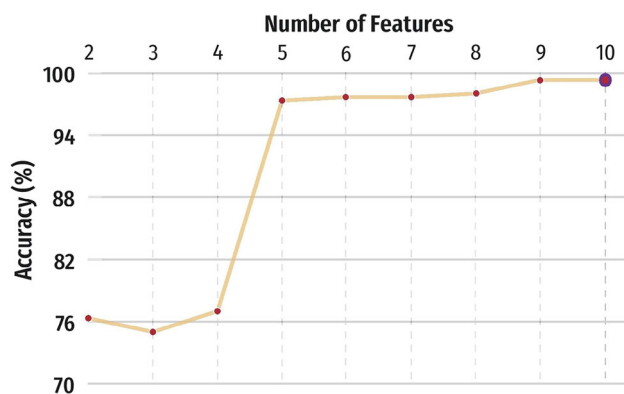
Kernel	TP	TN	FP	FN	Acc. (%)	PPV (%)	Sen. (%)	Spe. (%)
Poly order 1	148	150	0	2	99.33	100	98.66	100
Poly order 2	148	148	2	2	98.66	98.66	98.66	98.66
Poly order 3	145	138	12	5	94.33	92.35	96.66	92
RBF	130	147	3	20	92.33	97.74	86.66	98

Table 4 Performance evaluation using SVM classifier with different kernels using fifteen features (ten iterations)

Kernel	TP	TN	FP	FN	Acc. (%)	PPV (%)	Sen. (%)	Spe. (%)
Poly order 1	146	149	1	4	98.33	99.31	97.33	99.33
Poly order 2	146	147	3	4	97.66	97.98	97.33	98
Poly order 3	128	133	17	22	87	88.27	85.33	88.66
RBF	124	143	7	26	89	94.65	82.66	95.33

Table 5 Performance evaluation using SVM classifier with different kernels using twenty features (ten iterations)

Kernel	TP	TN	FP	FN	Acc. (%)	PPV (%)	Sen. (%)	Spe. (%)
Poly order 1	143	149	1	7	97.33	99.30	95.33	99.33
Poly order 2	143	145	5	7	96	96.62	95.33	96.66
Poly order 3	133	132	18	17	88.33	88.07	88.66	88
RBF	131	142	8	19	91	94.24	87.33	94.66

**Fig. 5** Accuracy of the proposed method for SVM with polynomial of order 1 using different features

The limitation of this work is that we have used only 50 normal and 50 CHF patients. Our system need to be tested with huge number of normal and CHF patients. Also, more early stage of CHF patients is to be used belonging to diverse background.

5 Conclusion and future work

This study focuses on the discrimination of normal and CHF patients caused due to DCM using US images. The proposed method achieved an average accuracy of 99.33% by combining VMD and texture features. This combination is able to capture the dissimilarity in the movements of four chambers of normal and CHF subjects. The obtained acceptable performance will prove that the proposed method can predict CHF caused due to DCM, and hence, the patients can undergo early treatment which may save their lives. Echocardiography can help to identify the CHF due to DCM in its initial asymptomatic phase which can benefit the patient to get early medication. Moreover, echocardiography-based diagnosis analyzes the structure and function of the heart which can indicate various cardiac abnormalities. In future, we intend to develop CAD tool for other cardiovascular diseases such as ischemic heart disease, congenital heart disease, valvular heart disease and systemic diseases. Also, we intend to develop a single

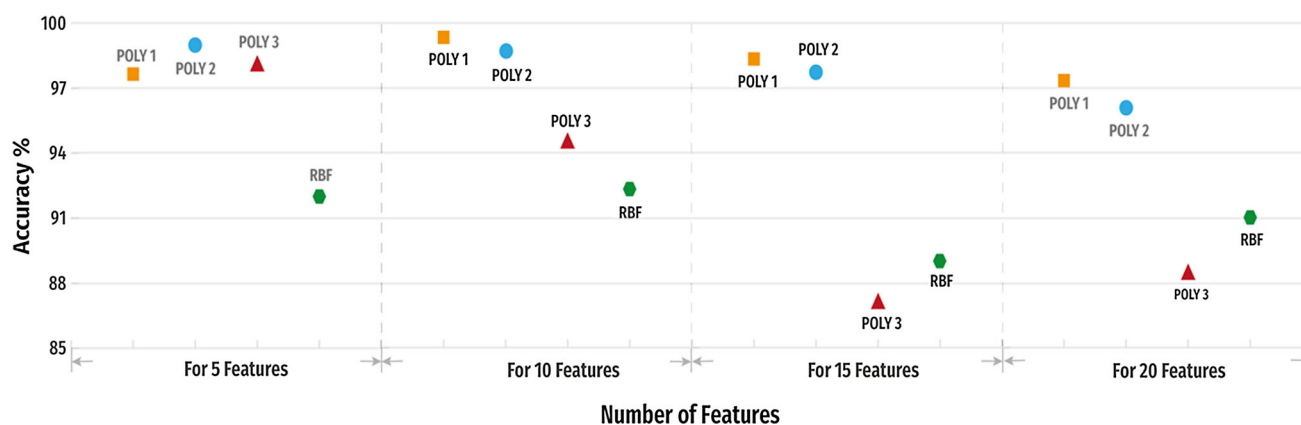


Fig. 6 Consolidated performance of kernel functions for different features

scalar value for the identification of CHF using huge diverse dataset.

Compliance with ethical standards

Conflict of interest None of the authors have any conflict of interest.

Appendix

See Table 6.

Table 6 Mean and standard deviation (SD) of the used ten features

Features	Normal		CHF	
	Mean	SD	Mean	SD
TX105	0.800	0.071	0.876	0.055
TX149	1.293	0.628	1.403	0.648
TX33	0.078	0.047	0.053	0.034
TX26	623.81	184.46	580.60	188.82
TX12	0.767	0.057	0.702	0.087
TX114	0.704	0.271	0.802	0.289
TX48	3.216	0.644	3.173	0.556
TX91	1.333	0.239	1.203	0.205
TX115	0.256	0.115	0.290	0.125
TX129	0.101	0.107	0.068	0.063

References

- Nichols M, Townsend N, Luengo-Fernandez R, Leal J, Gray A, Scarborough P, Rayner M (2012) European cardiovascular disease statistics 2012. Brussels, European Society of Cardiology, Sophia Antipolis, European Heart Network
- Mann DL, Zipes DP, Libby P, Bonow RO (2005) Braunwald's heart disease: a text book of cardiovascular medicine, 10th edn. W.B. Saunders, Philadelphia, p 1
- Wenger NK, Abelman WH, Roberts WC, Hurst JW (1990) The heart, arteries and veins, 7th edn. McGraw-Hill, New York
- Acharya UR, Kannathal N, Hua LM, Yi LM (2005) Study of heart rate variability signals at sitting and lying postures. *J Bodyw Mov Ther* 9(2):134–141
- Asyali MH (2003) Discrimination power of long-term heart rate variability measures. In: Engineering in medicine and biology society: proceeding of the 25th annual international conference of the IEEE EMBS, Cancun
- Isler Y, Kuntalp M (2007) Combining classical HRV indices with wavelet entropy measures improves to performance in diagnosing congestive heart failure. *Comput Biol Med* 37:1502–1510
- Hossen A, Al-Ghunaimi B (2007) A wavelet-based soft decision technique for screening of patients with congestive heart failure. *Biomed Signal Process Control* 2:135–143
- Pecchia L, Melillo P, Sansone M, Bracale M (2011) Discrimination power of short-term heart rate variability measures for CHF assessment. *IEEE Trans Inf Technol Biomed* 15(1):40–46
- Yu S-N, Lee M-Y (2012) Conditional mutual information-based feature selection for congestive heart failure recognition using heart rate variability. *Comput Methods Programs Biomed* 108(1):299–309
- Masetic Z, Subasi A (2016) Congestive heart failure detection using random forest classifier. *Comput Methods Programs Biomed* 130:54–64
- Acharya UR, Fujita H, Sudarshan VK, Oh SL, Muhammad A, Koh JEW, Tan JH, Chua CK, Chua KP, Tan RS (2016) Application of empirical mode decomposition (EMD) for automated identification of congestive heart failure using heart rate signals. *Neural Comput Appl*. doi:10.1007/s00521-016-2612-1
- Pai VB, Nahata MC (2000) Cardiotoxicity of chemotherapeutic agents: incidence treatment and prevention. *Drug Saf* 22(4):263–302
- Feigenbaum H, Armstrong WF, Ryan T (2004) Feigenbaum's echocardiography, 6th edn. Lippincott, Williams & Wilkins, Philadelphia
- Cleland JG, Dargie HJ, Ford I (1987) Mortality in heart failure: clinical variables of prognostic value. *Br Heart J* 58:572–582
- Wenger NK, Abelman WH, Roberts WC, Hurst JW (1990) The heart, arteries and veins, 7th edn. McGraw-Hill, New York, pp 1278–1347
- Middlekauff HR, Stevenson WG, Stevenson LW (1991) Prognostic significance of atrial fibrillation in advanced heart failure. A study of 390 patients. *Circulation* 84:40–48
- Williams JF (1995) Guidelines for the evaluation and management of heart failure. Report of the American College of Cardiology/American Heart Association Task Force on Practice

- Guidelines (Committee on Evaluation and Management of Heart Failure). *J Am Coll Cardiol* 26:1376–1398
18. Solomon SD, Anavekar N, Skali H, McMurray JJV, Swedberg K, Yusuf S, Granger CB, Michelson EL, Wang D, Pocock S, Pfeffer MA (2005) Influence of ejection fraction on cardiovascular outcomes in a broad spectrum of heart failure patients. *Circulation* 112(24):3738–3744
 19. Zuiderveld K (1994) Contrast limited adaptive histogram equalization, graphic gems IV. Academic Press Professional, San Diego, pp 474–485
 20. Keys R (1981) Cubic convolution interpolation for digital image processing. *IEEE Trans Acoust Speech Signal Process* 29(6):1153–1160
 21. Dragomiretskiy K, Zosso D (2015) Two dimensional variational mode decomposition. In: 10th international conference, EMMCVPR, pp 197–208
 22. Hestenes MR (1969) Multiplier and gradient methods. *J Optim Theory Appl* 4(5):303–320
 23. Rockafellar RT (1973) A dual approach to solving nonlinear programming problems by unconstrained optimization. *Math Program* 5(1):354–373
 24. Bertsekas DP (1982) Constrained optimization and lagrange multiplier methods, vol 1. Academic Press, Boston
 25. Hassanpour H, Samadiani N, Salehi SMM (2015) Using morphological transforms to enhance the contrast of medical images. *Egypt J Radiol Nucl Med* 46(2):481–489
 26. Haralick RM, Shanmugam K, Dinstein I (1973) Textural features of image classification. *IEEE Trans Syst Man Cybern* 3(6):610–621
 27. Soh L, Tsatsoulis C (1999) Texture analysis of SAR sea ice imagery using gray level co-occurrence matrices. *IEEE Trans Geosci Remote Sens* 37(2):780–795
 28. Clausi DA (2002) An analysis of co-occurrence texture statistics as a function of grey level quantization. *Can J Remote Sens* 28(1):45–62
 29. Acharya UR, Chua KC, Ng EYK, Wei W, Chee C (2008) Application of higher order spectra for the identification of diabetes retinopathy stages. *J Med Syst* 32(6):481–488
 30. Acharya UR, Dua S, X Du, Chua CK (2011) Automated diagnosis of glaucoma using texture and higher order spectra features. *IEEE Trans Inf Technol Biomed* 15(3):449–455
 31. Weszka JS, Rosenfield A (1976) An application of texture analysis to material inspection. *Pattern Recognit* 8(4):195–200
 32. Galloway MM (1975) Texture classification using gray level run length. *Comput Graph Image Process* 4(2):172–179
 33. Kennedy J, Eberhart R (1995) Particle swarm optimization. *Proc IEEE Int Conf Neural Netw* 4:1942–1948
 34. Shi Y, Eberhart R (1998) A modified particle swarm optimizer. In: *Proceedings of IEEE International CEC*, pp 69–73
 35. Kecman V (2001) Learning and soft computing. MIT Press, Cambridge
 36. Salzberg SL (1997) On comparing classifiers: pitfalls to avoid and a recommended approach. *Data Min Knowl Discov* 1(3):317–328
 37. Lin S-W, Ying K-C, Chen S-C, Lee Z-J (2008) Particle swarm optimization for parameter determination and feature selection of support vector machines. *Expert Syst Appl* 35:1817–1824
 38. Acharya UR, Sree SV, Krishnan MMR, Molinari F, Saba L, Ho SYS, Ahuja AT, Ho SC, Nicolaides A, Suri JS (2012) Atherosclerotic risk stratification strategy for carotid arteries using texture-based features. *Ultrasound Med Biol* 38(6):899–915
 39. Acharya UR, Ng EYK, Tan JH, Sree SV, Ng K-H (2012) An integrated index for the identification of diabetic retinopathy stages using texture parameters. *J Med Syst* 36(3):2011–2020
 40. Raghavendra U, Acharya UR, Fujita H, Gudigar A, Tan JH, Chokkadi S (2016) Application of gabor wavelet and locality sensitive discriminant analysis for automated identification of breast cancer using digitized mammogram images. *Appl Soft Comput* 46:151–161